ACS OMEGA

http://pubs.acs.org/journal/acsodf

Article

Computational Modeling of the Interaction of Silver Clusters with Carbohydrates

Felipe E. Gallegos, Lorena M. Meneses,* Sebastián A. Cuesta, Juan C. Santos, Josefa Arias, Pamela Carrillo, and Fernanda Pilaquinga

Cite This: *ACS Omega* 2022, 7, 4750−4756

Read Online

ACCESS | Metrics & More | Article Recommendations | Supporting Information

ABSTRACT: Silver nanoparticles are recognized for their numerous physical, biological, and pharmaceutical applications. In the present study, the interaction of silver clusters with monosaccharide molecules is examined to identify which molecule works better as a reducing agent in the application of a green synthesis approach. Geometry optimization of clusters containing one, three, and five silver atoms is performed along with the optimization of α-D-glucose, α-D-ribose, D-erythrose, and glyceraldehyde using density functional theory. Optimized geometries allow identifying the interaction formed in the silver cluster and monosaccharide complexes. An electron localization function analysis is performed to further analyze the interaction found and explain the reduction process in the formation of silver nanoparticles. The overall results indicate that glyceraldehyde presents the best characteristics to serve as the most efficient reducing agent.

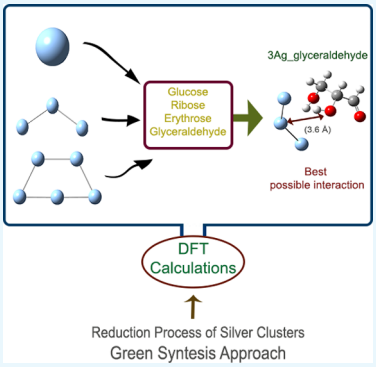

INTRODUCTION

In the last few decades, nanoscience and its applications have greatly advanced in the field of chemistry.[1] Silver nanoparticles (Ag-NPs) have been widely studied and are one of the most used in nanoscience research and industry due to their easy and fast production.[2] Ag-NPs can be synthesized by physical and chemical means. However, green synthesis is considered the safest and less toxic alternative to obtain them.[3] Furthermore, the method has been strongly accepted as it reduces toxicity levels and allows better biocompatibility.[4] Ag-NPs have numerous applications, including medicinal ones such as biomolecular detection and drug delivery carriers. They also serve as an antibacterial, antiviral, and antifungal agent.[5,6]

Green synthesis methods usually take advantage of biological systems like microorganisms, plants, bacteria, enzymes, or common sugars to act as reducing agents.[7,8] Monosaccharides (MS) are molecules whose structure comprises a large percentage of oxygen atoms, which can reduce different metal ions including silver. Therefore, sweeteners like white sugar, honey, and brown sugar have been used to obtain Ag-NPs.[9]

Density functional theory (DFT) is a quantum-mechanical method that assesses molecular properties in simple and complex chemical systems. DFT computational codes determine accurate approximations of electronic structures of ground states, kinetics, and thermodynamics properties as well as minima on potential energy surfaces, geometry optimizations, and others.[10] In conjunction with DFT calculations, noncovalent interactions (NCI), atoms in molecules (AIM), and electron localization function (ELF) have emerged as quantum chemical tools that allow comprehending physical and chemical properties in nonbonding interactions just as the ones that take place between silver and carbohydrate molecules.[11−13]

Computational modeling is a powerful tool that can help gain insights at a molecular level about the interactions involved in the silver reduction to form Ag-NPs, something that cannot be done through common experimental essays.[14] This can lead to determining which carbohydrate will produce a more efficient reduction of silver ions. In previous studies, computational modeling has been used to obtain geometric and electronic structure predictions for gold and Ag-NPs.[15,16] Similarly, Fabara et al.[17] used molecular dynamics (MD) and DFT methods to study silver-atom clusters and their behavior with compounds found in the skin's lipid layer. In this case, DFT helped to determine compounds' stability, while MD revealed that Ag-NPs had good clearance properties due to weak interactions with fatty acids.

The present study aims to identify which MS is the most suitable reducing agent to perform a green synthesis of Ag-NPs. Studying different types of carbohydrates will provide information and understanding at a molecular level about interactions occurring during this process and determine which

Received: August 3, 2021
Accepted: December 23, 2021
Published: February 4, 2022

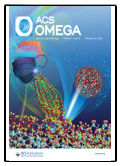

https://doi.org/10.1021/acsomega.1c04149
ACS Omega 2022, 7, 4750−4756

one presents better properties to reduce silver atoms into Ag-NPs.[18] Clusters of one, three, and five silver atoms were chosen based on Fabara et al.'s work.[17] Moreover, α-D-glucose, α-D-ribose, D-erythrose, and D-glyceraldehyde (from now on called just glucose, ribose, erythrose, and glyceraldehyde) were chosen as reducing agents (Figure 1). An ELF analysis was also performed to evaluate the interactions occurring when the Ag_MS complex is formed.

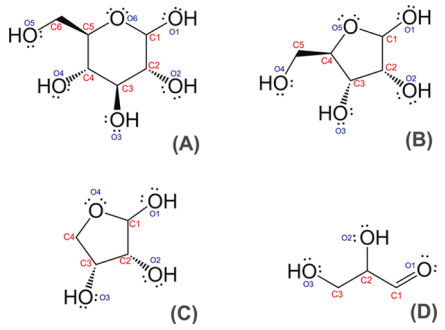

Figure 1. Lewis's structure and numbering scheme used for definition in all studied structures; glucose (A), ribose (B), erythrose (C), and glyceraldehyde (D).

RESULTS AND DISCUSSION

To study the different complexes, all of the structures were optimized. Figure 2 shows the optimized structures of the three silver clusters. To find the most stable clusters, several conformations were tested (Figures S1 and S2) and their energies compared (Table S1). The most stable three-silver-atom cluster presents equal bond lengths of 2.7 Å and forms a 122.5° angle (Figure 2B). Its estimated energy is 0.45 kcal/mol lower than the second most stable conformation. Results were compared to Dale et al.'s[19] study, which proposes a linear conformation to be the one with the lowest energy. When testing the linear conformation, an energy value of 3.5 kcal/mol higher was found, compared to the lowest energy conformation obtained in this study. The variation found regarding the conformation of the three-silver-atom cluster may be attributed to a difference in the functional used during the optimization process (BP86 vs B3LYP) or that the conformation found in this study was not tested.

For the most stable five-silver-atom cluster (Figure 2C), all bonds were found to have the same length (2.8 Å) forming two angles of 61.5°. The energy found is 5.72 kcal/mol lower than the second most stable conformation (Table S1A) and 13.90 kcal/mol lower than the nonplanar conformation, which is the least stable structure found (Table S1D). In a five-silver-atom cluster, there is the possibility to form different conformations, including nonplanar ones, due to an increase in the number of atoms. From the tested conformations, our findings are closely related to other literature, which suggest the same stable structures.[20−22]

Itoh et al.[20] determined that planar conformations are more stable between three to six silver atom clusters. In clusters containing six to seven silver atoms, this stabilization changed from planar to nonplanar conformations. Results showed that nonplanar conformations are less stable than planar conformations agreeing with Itoh et al.'s[20] findings. In the five-silver-atom cluster, its planar structure can be verified by measuring its dihedral angles (0°). As silver clusters increase their size (number of atoms per particle), they tend to generate a quasi-spherical morphology, such as cuboctahedral or pentagonal rods.[20,23,24] This behavior can be seen in the five-silver-atom cluster in which their atoms start closing and reducing their angles compared to the three-silver-atom cluster.

Carbohydrates, especially aldoses, possess aldehydes groups in their structure. These grant them the ability to oxidize easily to carboxylic acids, while reducing the oxidizing agents involved; in this case, silver atoms.[25] As shown in Figure 1, in an aqueous environment, glucose, ribose, and erythrose are cyclic molecules with hemiacetal groups. Therefore, the carbonyl group is not there anymore, leaving only hydroxyl groups and ether.[25] In the case of glyceraldehyde, its size impedes a cyclic formation.[26]

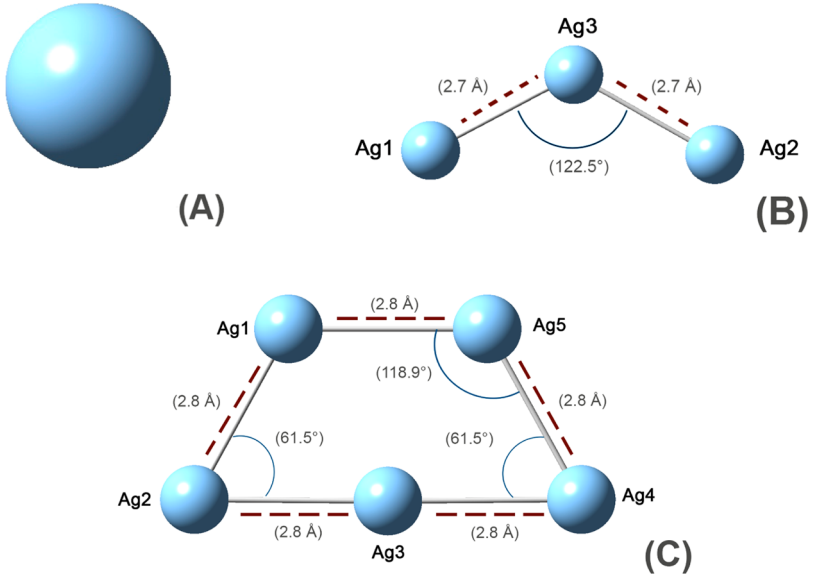

Figure 2. Most stable conformations for single silver atom (A), cluster of three silver atoms (B), and a cluster of five silver atoms (C). Additionally, the enumeration scheme is used in clusters (B) and (C) for definition purposes.

https://doi.org/10.1021/acsomega.1c04149
ACS Omega 2022, 7, 4750−4756

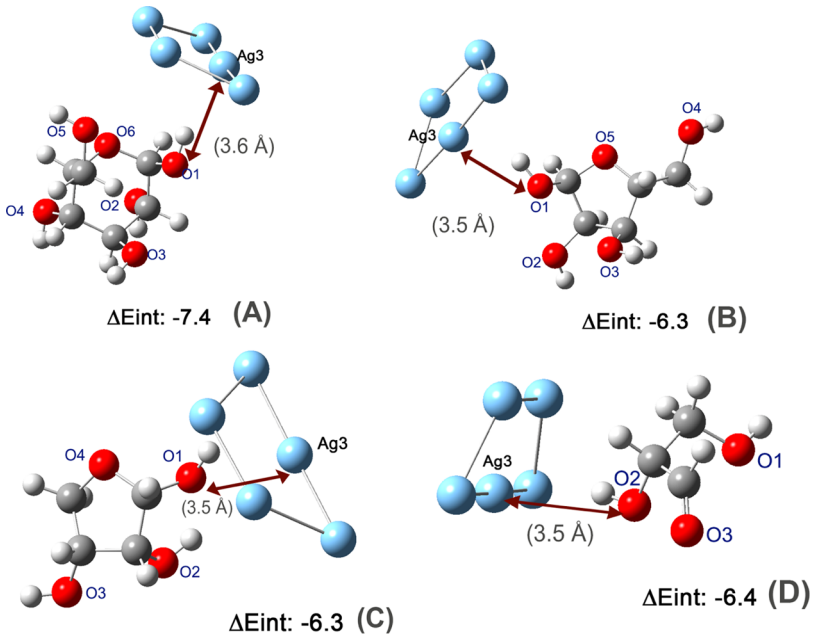

Figure 3. Most stable geometries and interaction energies (ΔE_{int}) of the five-silver-atom cluster complexed with (A) glucose, (B) ribose, (C) erythrose, and (D) glyceraldehyde molecules.

The interaction between the MS molecules and the silver clusters was modeled and their configuration optimized to determine whether both structures could form a complex. Based on the information provided by He and Zeng,[27] the silver atom and the clusters should be placed close to the oxygen atoms, which are basic centers. To determine which oxygen atom will produce the most stable complex, different one-silver-atom-MS complexes were built, changing the silver position around the carbohydrate molecule. Once the most stable position was found, the same arrangement was applied to the different Ag_MS complexes.

The charge distribution of the carbohydrate's molecules is governed by oxygen atoms. These sites are considered the most active since they can donate electron density to the silver atoms. In this sense, one electron might be transferred to the silver atom to pass from a Ag^+ cation to Ag^0, filling up $5s^2$ and $4d^9$ orbitals.[26,28] For this process to happen, both atoms should be in contact; therefore, the distance between the silver cluster atoms and the carbohydrate molecule is key when studying these systems. For a complex formation, distances represent an important factor and reflect the type of interactions. For comparison purposes, a normal oxygen−silver bond (silver oxide) distance is about 2.31 Å.[29]

Ag_MS distances were measured to determine how close they get and evaluate the type of interaction.[30] To compare distances, the most centric silver atom in each cluster was selected (silver atom number Ag3). Results showed that all silver clusters have a major closeness to O1 in glucose, ribose, erythrose, and O2 in glyceraldehyde, following the numeric scheme shown in Figure 1.

Figure 3 shows the most stable complexes formed by the five-silver-atom cluster with the four different MS and their interaction energies (ΔE_{int}). As seen throughout these optimized geometries, silver clusters arranged themselves to get the most interaction possible with the MS. The distances with the hydroxyl group are 3.6 Å in glucose and 3.5 Å in ribose, erythrose, and glyceraldehyde. Optimized complexes formed with one-and-three-silver atom clusters are displayed in the Supporting Information (Figures S3 and S4). One-silver-atom cluster distances are 3.6 Å for glucose and ribose and 3.5 Å for erythrose and glyceraldehyde. For the most stable complexes in the three-silver-atom cluster group, the distances are bigger than the ones found for the one-and-five-silver-atom clusters being 3.7 Å in ribose and 3.6 Å in glucose, erythrose, and glyceraldehyde.

For one-silver-atom complexes, their interaction energies were the highest, ranging from −3.2 to −2.8 kcal/mol, while their distances were the shortest. This suggests poor interaction due to fewer silver atoms. Energies of three-silver-atom complexes present a value of −5.4 and −8.4 kcal/mol for glucose and glyceraldehyde, respectively, while their distances were longer than the estimated in the one-silver-atom complexes. Complexes with the five-silver-atom cluster had the lowest interaction energies among the 12 studied systems, specifically, glyceraldehyde and glucose with −6.4 and −7.4 kcal/mol, respectively. This suggests favorable binding between the five-silver-atom clusters and the MS, while their distances were similar to the three-silver-atom complexes.

It seems that as the complexes grow in the number of silver atoms, distances reach an average length (Figures S4 and 3), and interaction energies decrease. Lower energy values are mainly influenced by the type of carbohydrate that is used, leading to better interactions and more stabilized complexes. Results showed that glyceraldehyde has the lowest distances and interaction energies among all, which may suggest better reducing activity.

The interaction between an organic molecule and a nanoparticle (NP) will depend on the nature of the molecule and the size of the NP.[31] Although one silver atom could interact more intimately with the MS, it cannot interact with different zones of the molecule as the three- and five-silver-atom clusters do, which can result also in a better interaction.[32]

The complex formation energy (ΔE_{BE}) was obtained from the optimized complexes and is presented in Table 1. Furthermore, the distortion and interaction energies are

https://doi.org/10.1021/acsomega.1c04149
ACS Omega 2022, 7, 4750−4756

tabulated for the set of Ag_MS complexes obtained in this study.

Table 1. Complex Formation Energy ΔE_{BE}, Distortion Energies ΔE_{dist} (Ag_n) and ΔE_{dist} (MS), and Interaction Energy ΔE_{int} (in kcal/mol) between distorted species for different studied complexes

complex	ΔE_{BE}	ΔE_{dist} (Ag_n)	ΔE_{dist} (MS)	ΔE_{int}
1Ag_glucose	2.2		5.4	−3.2
1Ag_ribose	1.7		4.6	−2.9
1Ag_erythrose	1.0		3.8	−2.8
1Ag_glyceraldehyde	2.2		5.0	−2.8
3Ag_glucose	0.3	0.0	5.7	−5.4
3Ag_ribose	−1.6	0.1	4.9	−6.6
3Ag_erythrose	−1.4	0.0	4.0	−5.3
3Ag_glyceraldehyde	−3.7	0.0	4.7	−8.4
5Ag_glucose	−1.4	0.0	5.9	−7.4
5Ag_ribose	−1.4	0.0	4.8	−6.3
5Ag_ erythrose	−2.2	0.0	4.1	−6.3
5Ag_glyceraldehyde	−0.9	0.0	5.4	−6.4

Results showed that the complexes formed with clusters of three-and-five-silver-atoms are thermodynamically more favored than the ones produced with the single silver atom;[33] all one-silver-atom complexes obtained positive formation energies. When analyzing each monosaccharide, inside the groups of three-and-five-silver-atoms complexes, glucose is the only one that presents positive complex formation energy in the complex formed with the three-silver-atom cluster; its most favorable complex is the one formed with the five silver atoms (−1.4 kcal/mol). Similar behavior is observed within the erythrose complexes, where the most favorable one occurs between the MS and the five-silver-atom cluster (−2.2 kcal/mol). Interestingly, for glyceraldehyde and ribose, the three-silver-atom cluster is the one that produces the most stable complexes. Comparing all of the 12 systems, 3Ag glyceraldehyde is the most favorable one with a complex formation energy of −3.7 kcal/mol. This may be because glucose, erythrose, and ribose are cycled in aqueous solvents. The MS cyclization reaction forms a hemiacetal, where the carbonyl group is not available to be easily oxidized.[25] On the other hand, due to the size and structure of glyceraldehyde, the oxidation−reduction reaction takes place easily.

An ELF analysis was performed to get insights into the Ag_MS interaction. Figure 4 shows the decomposition energy scheme used to establish which role is played in each contribution in the formation of the Ag_MS complex.

Results show that the contribution of the silver clusters is negligible to the complex formation, ΔE_{dist} (Ag_n). Looking at the optimized structures, the negligible contribution can be explained because the clusters did not suffer appreciable structural deformation or geometric distortion in the formation of the studied complexes. On the other hand, the MS structures presented structural deformation, which causes the distortion energy of these structures to be around 5 kcal/mol. The formation of highly stabilized complexes can be observed by the negative values obtained for the complex formation energy (ΔE_{BE}) of the systems, which is accompanied by higher values of ΔE_{dist} (MS). This favors a stronger interaction between distorted species, which obtained negative ΔE_{int} values.

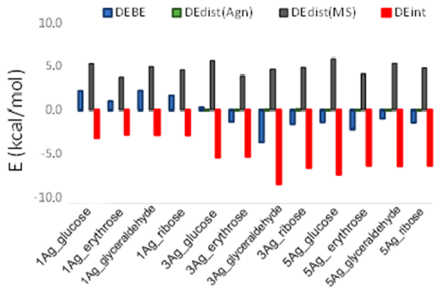

Figure 4. Energy contribution of all of the studied systems. Negative interaction energies reflect strong interactions for all complexes, particularly 3Ag_glyceraldehyde. Positive distortion energies were found for both Ag and MS. Negative values for all complex formation energies were expected; however, only complexes of one-silver-atom cluster obtained positive data.

Finally, Figure 5 shows the representation of the ELF basins of all of the studied systems. In the figures, the most relevant bonds in the studied complexes can be visualized. A typical characterization of the Lewis representation for C−C, C−H, and C−O bonds and lone pairs on the oxygen atom of the MS structures can be appreciated. The most important fact is that bond formation, between silver clusters and monosaccharides, was not observed in any of the studied complexes, which suggests that the oxidation/reduction process only involves interactions and charge transfer but not a proper bond formation.

CONCLUSIONS

A DFT approach was used to simulate, at a molecular level, the interaction process between silver clusters and four MS to determine which one presents the better properties to reduce silver ions and form Ag-NPs. As seen in the optimized structures, the one-silver-atom cluster presents the closest distances during the interaction with all of the MS. Results showed that D-erythrose and D-glyceraldehyde present the shortest distances with all of the silver clusters, being 3.5 Å for both molecules. Moreover, complexes between the five-silver-atom cluster and MS, glyceraldehyde, and glucose were the most stable structures as they presented the lowest interaction energies in this study (−7.4 and −6.4 kcal/mol, respectively). Furthermore, the lowest complex formation energy was found for the 3Ag_D-glyceraldehyde complex with a value of −3.7 kcal/mol. ELF analysis concludes that the silver reduction process does not involve any bond formation and only nonbonding interactions. These results give an idea of the performance of these carbohydrates, where D-glyceraldehyde, the most stable complex, seems to be the best candidate as a reducing agent in the green synthesis of Ag-NPs.

COMPUTATIONAL METHODS

To study the interaction between silver clusters and carbohydrate molecules, 12 systems were built. One-, three-, and five-silver-atom clusters were selected to interact with each of the four carbohydrate molecules considered in this study (glucose, ribose, erythrose, and glyceraldehyde). All of the structures including the silver clusters, monosaccharides (MS), and complexes (Ag_MS) formed between them were optimized and their vibrational frequencies obtained.[4,34]

Calculations were performed using a polarizable continuum model (PCM) of water including in the solvation model density (SMD) approach implemented in Gaussian 09W

https://doi.org/10.1021/acsomega.1c04149
ACS Omega 2022, 7, 4750−4756

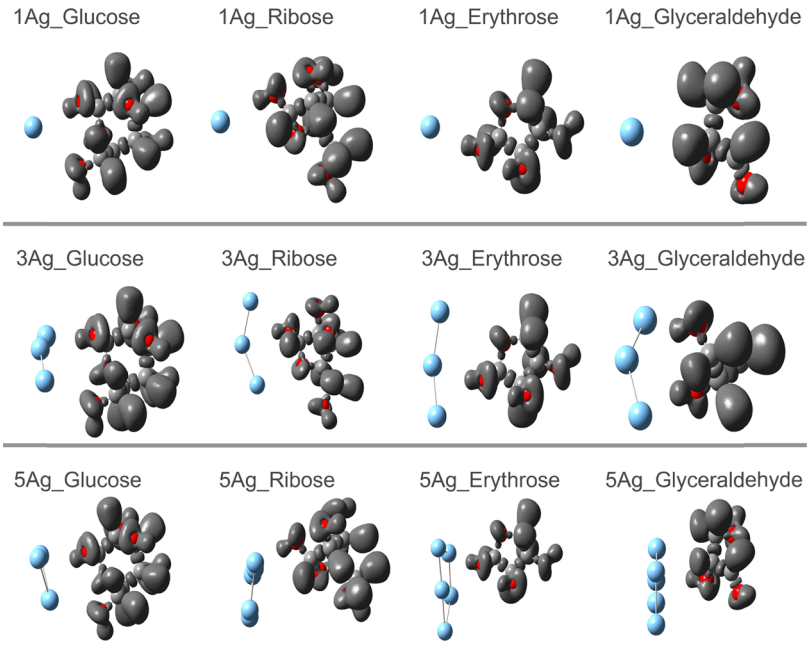

Figure 5. ELF isosurfaces (ELF = 0.75) of studied complexes.

software.[35] The Becke's three-parameter functional and the Lee−Yang−Parr hybrid functional B3LYP level of calculation was employed. The B3LYP functional has been previously used to study Ag-NPs;[17,36,37] additionally, it delivers stable geometry configurations and reproducible results.[38,39] The LANL2DZ basis set[40] was used for silver atoms, as it describes first-row transition metals[41,42] and the 6−311g(d,p) basis set for the organic systems.[43] This mixed basis set was used for the 12 complexes (Ag_MS), as it improves thermodynamic parameters.[44,45] The ELF analysis was made using the Multiwfn program,[46] and its graphical representation was obtained using GaussView6 software.[47]

First, different conformations for the three-silver-atom cluster and five-silver-atom cluster including planar and nonplanar configurations were tested to find the most stable conformation. In parallel, MS molecules were built and optimized. Then, the one-silver-atom cluster was used to form different Ag_MS configurations with all of the studied MS to establish the position in which the single silver atom forms the most stable complex. To achieve this, optimization calculations were made combining the B3LYP functional and the mixed basis set. From this information, complexes (Ag_MS) were formed with the rest of the silver cluster structures and then optimized utilizing the same functional and mixed basis set. Finally, the electron localization function (ELF)[48] tool was used as it assesses the presence or the absence of a bond between silver clusters and MS in the different complexes, where the gradient vector field of ELF divides the space in basins of attractors where electron pairs are located.

The complex formation energy ΔE_{BE} of each of the 12 systems was calculated, as described in eq 1.

$$\Delta E_{BE} = E_{CX} - [E_{Ag_n} + E_{MS}] \quad \text{where } n = 1, 3, 5 \text{ silver atoms} \tag{1}$$

Afterward, following a two-step process, as shown in Figure 6, an energy partition known as strain/interaction[49] or distortion/interaction model[50] was applied. This method has been successfully employed to surface adsorption in the limit of low coverage by Scaranto et al.[51] To achieve this, both Ag_n and MS structures are distorted in their complex geometries in the first stage allowing them to interact in a second one. With these calculations, ΔE_{BE} can be decomposed into two contributions, as shown in eq 2.

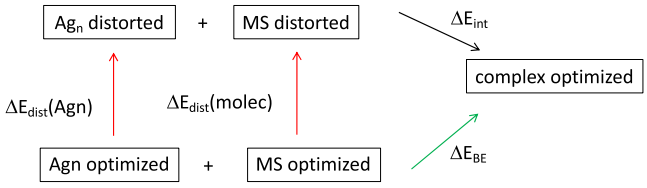

Figure 6. Energy partition protocol following the distortion/interaction model.

$$\Delta E_{BE} = \Delta E_{dist} + \Delta E_{int} \tag{2}$$

The distortion energy (ΔE_{dist}) is calculated by adding the distortion energy of the Ag_n and the MS, as shown in eq 3. The energies required to distort reactants (Ag_n or MS) can be calculated as the difference between the energy of the isolated deformed complex (using the geometry in the complex) and the energy of the optimized ground state of the isolated cluster or monosaccharide, respectively (eq 4).

$$\Delta E_{dist} = \Delta E_{dist}(Ag_n) + \Delta E_{dist}(MS) \tag{3}$$

$$\Delta EX_{dist} = EX_{distorted} - EX_{optimized} \quad X = Ag_n, MS \tag{4}$$

Finally, the process of complex formation from distorted reactants releases an energy known as interaction energy (ΔE_{int}), which can be calculated using eq 5.

$$\Delta E_{int} = E_{CX} - (E_{Ag_n,distorted} + E_{MS,distorted}) \tag{5}$$

ΔE_{int} can also be computed in an easier way in terms of ΔE_{BE} and ΔE_{dist} (eq 6).

https://doi.org/10.1021/acsomega.1c04149
ACS Omega 2022, 7, 4750−4756

$$\Delta E_{int} = \Delta E_{BE} - \Delta E_{dist} \quad (6)$$

■ ASSOCIATED CONTENT

Supporting Information

The Supporting Information is available free of charge at https://pubs.acs.org/doi/10.1021/acsomega.1c04149.

All tested conformations, including nonplanar configurations, were used in this study to determine the most stable structures of three- and five-silver-atom clusters; minimal energies of each system compared with the most stable silver cluster conformation; and optimized complexes of three- and five-silver-atoms with their respective studied monosaccharides (PDF)

■ AUTHOR INFORMATION

Corresponding Author

Lorena M. Meneses − *Laboratory of Computational Chemistry, Chemical Science Department, Pontificia Universidad Católica del Ecuador, Quito 170143, Ecuador;* orcid.org/0000-0002-1517-5247; Email: lmmeneses@puce.edu.ec

Authors

Felipe E. Gallegos − *Laboratory of Computational Chemistry, Chemical Science Department, Pontificia Universidad Católica del Ecuador, Quito 170143, Ecuador*

Sebastián A. Cuesta − *Laboratory of Computational Chemistry, Chemical Science Department, Pontificia Universidad Católica del Ecuador, Quito 170143, Ecuador*

Juan C. Santos − *Ingeniería G-Mar LTDA, Peñalolén 7921490 Santiago, Chile*

Josefa Arias − *Laboratory of Computational Chemistry, Chemical Science Department, Pontificia Universidad Católica del Ecuador, Quito 170143, Ecuador*

Pamela Carrillo − *Chemistry Department, University of Liverpool, Liverpool L69 72D, United Kingdom*

Fernanda Pilaquinga − *Laboratory of Nanotechnology, Chemical Sciences Department, Pontificia Universidad Católica del Ecuador, Quito 17012184, Ecuador*

Complete contact information is available at: https://pubs.acs.org/10.1021/acsomega.1c04149

Notes

The authors declare no competing financial interest.

■ ACKNOWLEDGMENTS

This work was supported by the Pontificia Universidad Católica del Ecuador (PUCE).

■ REFERENCES

(1) Whitesides, G. M. Nanoscience, nanotechnology, and chemistry. *Small* **2005**, *1*, 172−179.

(2) Rai, M.; Yadav, A.; Gade, A. Silver nanoparticles as a new generation of antimicrobials. *Biotechnol. Adv.* **2009**, *27*, 76−83.

(3) Garibo, D.; Borbón-Nuñez, H.; Díaz de León, J.; Mendoza, E.; Estrada, I.; Toledano-Magaña, Y.; Tiznado, H.; Ovalle-Marroquin, M.; Soto-Ramos, A.; Blanco, A.; Rodríguez, J.; Romo, O.; Chávez-Almazán, L.; Susarrey-Arce, A. Green synthesis of silver nanoparticles using Lysiloma acapulcensis exhibit high-antimicrobial activity. *Sci. Rep.* **2020**, *10*, No. 12805.

(4) Akbari, M.; Morad, R.; Maaza, M. First principle study of silver nanoparticle interactions with antimalarial drugs extracted from *Artemisia annua plant*. *J. Nanoparticle Res.* **2020**, *22*, No. 331.

(5) Zhang, X.; Liu, Z.; Shen, W.; Gurunathan, S. Silver Nanoparticles: Synthesis, Characterization, Properties, Applications, and Therapeutic Approaches. *Int. J. Mol. Sci.* **2016**, *17*, 1534.

(6) Chavalmane, S.; Sakthi, D.; Khodakovskaya, M. *Plant Nanotechnology: Principles and Practices, Chapter 2*; Springer International Publishing, 2016; pp 15−27.

(7) Thakkar, K. N.; Mhatre, S. S.; Parikh, R. Y. Biological synthesis of metallic nanoparticles. *Nanomedicine* **2010**, *6*, 257−262.

(8) Lui, Y.-S.; Chang, Y.; Chen, H. Silver nanoparticle biosynthesis by using phenolic acids in rice husk extract as reducing agents and dispersants. *J. Food Drug Anal.* **2018**, *26*, 649−656.

(9) Hemmati, S.; Retzlaff, E.; Scott, C.; Harris, M. Artificial Sweeteners and Sugar Ingredients as Reducing Agent for Green Synthesis of Silver Nanoparticles. *J. Nanomater.* **2019**, *2019*, No. 9641860.

(10) Gázquez, J. L. Perspectives on the density functional theory of chemical reactivity. *J. Mex. Chem. Soc.* **2008**, *52*, 3−10.

(11) Johnson, E. R.; Keinan, S.; Mori-Sánchez, P.; Contreras-García, J.; Cohen, A.; Yang, W. Revealing Non-Covalent Interactions. *J. Am. Chem. Soc.* **2010**, *132*, 6498−6506.

(12) Kumar, P. S. V.; Raghavendra, V.; Subramanian, V. Bader's Theory of Atoms in Molecules (AIM) and its Applications to Chemical Bonding. *J. Chem. Sci.* **2016**, *128*, 1527−1536.

(13) Ishikawa, T. Ab initio quantum chemical calculation of electron density, electrostatic potential, and electric field of biomolecule based on fragment molecular orbital method. *Int. J. Quantum Chem.* **2017**, *118*, No. e25535.

(14) Vakhrouchev, A. V. Computer simulation of nanoparticles formation, moving, interaction and self-organization. *J. Phys.: Conf. Ser.* **2007**, *61*, 26−30.

(15) Aikens, C. Modelling small gold and silver nanoparticles with electronic structure methods. *Mol. Simul.* **2012**, *38*, 607−614.

(16) Poteau, R.; Heully, J.; Spiegelmann, F. Structure, stability, and vibrational properties of small silver cluster. *Z. Phys. D: At., Mol. Clusters* **1997**, *40*, 479−482.

(17) Fabara, A.; Cuesta, S.; Pilaquinga, F.; Meneses, L. Computational Modeling of the Interaction Silver Nanoparticles with the lipid layer of the Skin. *J. Nanotechnol.* **2018**, *2018*, No. 4927017.

(18) Jensen, F. *Introduction to Computational Chemistry*, 2nd ed.; John Wiley & Sons, Ltd., 2007.

(19) Dale, B. B.; Senanayake, R. D.; Aikens, C. M. Research Update: Density functional theory investigation of the interactions of silver nanoclusters with guanine. *APL Mater.* **2017**, *5*, No. 053102.

(20) Itoh, M.; Kumar, V.; Adschiri, T.; Kawazoe, Y. Comprehensive study of sodium, copper, and silver clusters over a wide range of sizes $2 \leq N \leq 75$. *J. Chem. Phys.* **2009**, *131*, No. 174510.

(21) Yang, M.; Jackson, K. A.; Jellinek, J. First-principles study of intermediate size silver clusters: Shape evolution and its impact on cluster properties. *J. Chem. Phys.* **2006**, *125*, No. 144308.

(22) Yang, M.; Jackson, K. A.; et al. Structure and shape variations in intermediate-size copper clusters. *J. Chem. Phys.* **2006**, *124*, No. 024308.

(23) Tak, Y. K.; Pal, S.; Naoghare, P.; Rangasamy, S.; Song, J. Shape-Dependent Skin Penetration of Silver Nanoparticles: Does It Really Matter? *Sci. Rep.* **2015**, *5*, No. 16908.

(24) Kelly, J.; Keegana, G.; Brennan-Fournet, M. Triangular Silver Nanoparticles: Their Preparation, Functionalisation and Properties. *Acta Phys. Pol., A* **2012**, *122*, 337−345.

(25) Clemens, R.; Jones, J.; Kern, M.; Soo-Yeun, L.; Mayhew, E.; Slavin, J.; Zivanovic, S. Functionality of Sugars in Foods and Health. *Compr. Rev. Food Sci. Food Saf.* **2016**, *15*, 433−470.

(26) Toxvaerd, S. The role of carbohydrates at the origin of homochirality in Biosystems. *Origins Life Evol. Biospheres* **2013**, *43*, 391−409.

(27) He, Y.; Zeng, T. First-Principles Study and Model of Dielectric Functions of Silver Nanoparticles. *J. Phys. Chem. C* **2010**, *114*, 18023−18030.

(28) Morad, R.; Akbari, M.; Rezaee, P.; Koochaki, A.; Maaza, M.; Jamshidi, Z. First principle simulation of coated hydroxychloroquine on Ag, Au and Pt nanoparticles. *Sci. Rep.* **2021**, *11*, No. 2131.
(29) Tavakol, H. Study of binding energies using DFT methods, vibrational frequencies and solvent effects in the interaction of silver ions with uracil tautomers. *Arabian J. Chem.* **2017**, *10*, S786−S799.
(30) Meneses-Olmedo, L.; Cuesta, S.; Moran, G.; Villada, W.; Candia, L.; Mendoza-Huizare, L. Insights on the mechanism, reactivity and selectivity of fructose and tagatose dehydration into 5-hydroxymethylfurfural: A DFT study. *Comput. Theor. Chem.* **2020**, *1190*, No. 113009.
(31) Chou, H. L.; Wu, C. M.; Lin, F. D.; Rick, J. Interactions between silver nanoparticles and polyvinyl alcohol nanofibers. *AIP Adv.* **2014**, *4*, No. 087111.
(32) De Jong, W.; Hagens, W.; Krystek, P.; Burgera, M.; Sips, A.; Geertsmad, R. Particle size-dependent organ distribution of gold nanoparticles after intravenous administration. *Biomaterials* **2008**, *29*, 1912−1919.
(33) Foroulan, M.; Khoee, S. MATLAB Applications in Behavior Analysis of Systems Consisting of Carbon Nanotubes through Molecular Dynamics Simulation. In *Computational Nanotechnology: Modeling and Applications with MATLAB*; Musa, S., Ed.; EEUU, 2012; pp 251−301.
(34) Shukla, M.; Verma, A.; Kumar, S.; Pal, S.; Sinha, I. Experimental and DFT calculation study of interaction between silver nanoparticle and 1-butyl-3-methyl imidazolium tetrafluoroborate ionic liquid. *Heliyon* **2021**, *7*, No. e06065.
(35) Frisch, M. J.; Trucks, G. W.; Schlegel, H. B.; Scuseria, G. E.; Robb, M. A.; Cheeseman, J. R.et al.*Gaussian 09*, Revision A.02; Gaussian Inc: Wallingford CT, 2009.
(36) Verma, A.; Gupta, R. K.; Shukla, M.; Malviya, M.; Sinha, I. Ag−Cu Bimetallic Nanoparticles as Efficient Oxygen Reduction Reaction Electrocatalysts in Alkaline Media. *J. Nanosci. Nanotechnol.* **2019**, *3*, 1765−1772.
(37) Verma, A.; Shukla, M.; Kumar, S.; Pal, S.; Sinha, I. Mechanism of visible light enhanced catalysis over curcumin functionalized Ag nanocatalysts. *Spectrochim. Acta, Part A* **2020**, *240*, No. 118534.
(38) Abroshan, H.; Li, G.; Lin, J.; Kim, H. J.; Jin, R. Molecular mechanism for the activation of Au25(SCH2CH2Ph)18 nanoclusters by imidazolium-based ionic liquids for catalysis. *J. Catal.* **2016**, *337*, 72−79.
(39) Contreras-Torres, F. F. Dispersion-Corrected Density Functional Theory Study of the Noncovalent Complexes Formed with Imidazo[1,2- a]pyrazines Adsorbed onto Silver Clusters. *ACS Omega* **2020**, *5*, 561−569.
(40) Becke, A. D. Density-functional thermochemistry. III. The role of exact exchange. *J. Chem. Phys.* **1993**, *98*, 5648−5652.
(41) Farshadfar, K.; Chipman, A.; Yates, B. F.; Ariafard, A. DFT Mechanistic Investigation into BF3-Catalyzed Alcohol Oxidation by a Hypervalent Iodine(III) Compound. *ACS Catal.* **2019**, *9*, 6510−6521.
(42) Check, C. E.; Faust, T. O.; Bailey, J. M.; Wright, B. J.; Gilbert, T. M.; Sunderlin, L. S. Addition of polarization and diffuse functions to the LANL2DZ basis set for P-block elements. *J. Phys. Chem. A* **2001**, *105*, 8111−8116.
(43) İnkaya, E. Synthesis, X-ray structure, FT-IR, NMR (13C/1H), UV−Vis spectroscopy, TG/DTA study and DFT calculations on 2-(benzo[d]thiazol-2-ylthio)-1-((1s, 3s)-3-mesityl-3-methylcyclobutyl) ethan-1-one. *J. Mol. Struct.* **2018**, *1173*, 148−156.
(44) Avcı, D.; Altürk, S.; Sönmez, F.; Tamera, Ö.; Başoğlu, A.; Atalay, Y.; Kurt, B.; Necmi, D. Three novel Cu(II), Cd(II) and Cr(III) complexes of 6−Methylpyridine−2−carboxylic acid with thiocyanate: Synthesis, crystal structures, DFT calculations, molecular docking and α-Glucosidase inhibition studies. *Tetrahedron* **2018**, *74*, 7198−7208.
(45) Yang, Y.; Weaver, N. M.; Merz, K. M. Assessment of the "6-31+G** + LANL2DZ" Mixed Basis Set Coupled with Density Functional Theory Methods and the Effective Core Potential: Prediction of Heats of Formation and Ionization Potentials for First-Row-Transition-Metal Complexes. *J. Phys. Chem. A* **2009**, *113*, 9843−9851.
(46) Lu, T.; Chen, F. Multiwfn: A multifunctional wavefunction analyzer. *J. Comput. Chem.* **2012**, *33*, 580−592.
(47) Dennington, R.; Keith, T. A.; Millam, J. M. *GaussView*. Version 6 Shawnee Mission, KS: Semichem Inc., 2016.
(48) Becke, A. D.; Edgecombe, K. E. A simple measure of electron localization in atomic and molecular systems. *J. Chem. Phys.* **1990**, *92*, 5397−5403.
(49) Bickelhaupt, F. M. Understanding reactivity with Kohn-Sham molecular orbital theory: E2−SN2 mechanistic spectrum and other concepts. *J. Comput. Chem.* **1999**, *20*, 114−128.
(50) Ess, D. H.; Houk, K. N. Distortion/interaction energy control of 1,3-dipolar cycloaddition reactivity. *J. Am. Chem. Soc.* **2007**, *129*, 10646−10647.
(51) Scaranto, J.; Mallia, G.; Harrison, N. M. An efficient method for computing the binding energy of an adsorbed molecule within a periodic approach. The application to vinyl fluoride at rutile TiO2(110) surface. *Comput. Mater. Sci.* **2011**, *50*, 2080−2086.

https://doi.org/10.1021/acsomega.1c04149
ACS Omega 2022, 7, 4750−4756